Journal of Sound and Vibration (2002) **254**(1), 23–36
doi:10.1006/jsvi.2001.4059, available online at http://www.idealibrary.com on IDEAL®

OPTIMIZATION OF ANISOTROPIC SANDWICH BEAMS FOR HIGHER SOUND TRANSMISSION LOSS

P. THAMBURAJ AND J. Q. SUN

Department of Mechanical Engineering, University of Delaware, Newark, DE 19716, *U.S.A.*

(*Received* 29 *May* 2001, *and in final form* 10 *October* 2001)

This paper presents a study on the optimization of sound transmission loss across anisotropic sandwich beams. It has been found in earlier studies that there is a significant increase in the sound transmission loss for sandwich beams with anisotropic materials compared to those with isotropic ones. The optimization studies presented in this work further validate this concept. The material and geometric properties of the structure are treated as the design variables with the objective to maximize the sound transmission loss across the beam. Appropriate constraints are imposed to maintain material and structural integrity.

1. INTRODUCTION

Composite sandwich structures have the unique feature that by adjusting the material and geometric properties of the skins and the core, various structures can be optimally created for specific applications [1–3]. Hence, optimization studies of these structures with respect to their material and geometric properties have been an important topic of research for a few decades. Most of these studies have been related to strength and buckling optimization issues [4–16]. There are relatively fewer studies on sandwich structures with optimal sound transmission characteristics [17–21].

The sound transmission loss across sandwich panels has been studied in detail by Dym and Co-workers [17, 18]. The optimal acoustic design of these panels have also been investigated [19, 20]. It was shown that the average transmission loss of a panel may be improved by optimization over a range of frequencies. The panels used in these studies are isotropic and the design variables for the optimization are Young's modulus, mass density and thicknesses of the skins and the core. There are few studies in the literature on the sound transmission characteristics of structures made of anisotropic materials. Humphrey and Chinnery studied the propagation of ultrasound in fiber-reinforced laminates [1], while Liu and colleagues examined harmonic wave propagation in anisotropic laminated strips [22].

This paper presents a study on the optimization of sound transmission loss across an anisotropic sandwich beam. It has been found in earlier studies that there is a significant increase in the sound transmission loss for sandwich beams with anisotropic materials than those with isotropic ones [23, 24]. The optimization studies presented in this work further validate this concept. The present work is based on the model developed in references [23, 24], where a highly efficient set of computer programs has been developed that are suitable for optimization studies.

0022-460X/02/$35.00

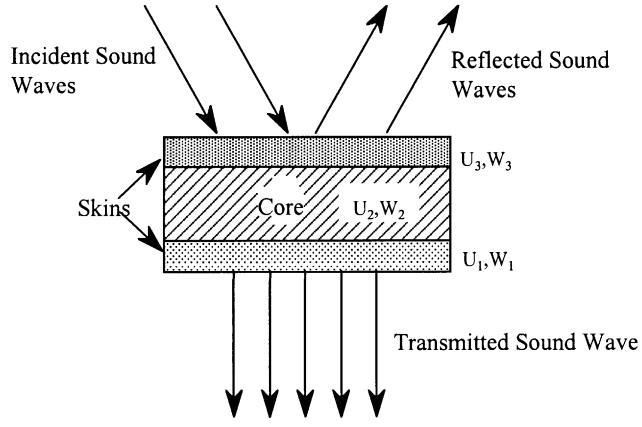

Figure 1. All illustration of sound transmission through a sandwich partition.

In this paper, the material and geometric properties of the structure are treated as the design variables. The objective of optimization is to maximize the sound transmission loss across the beam. Appropriate constraints are imposed on the mass of the sandwich structure as well as on the other design parameters in order to maintain material and structural integrity. A brief overview of the model of the sandwich beam in references [23, 24] is presented in section 2. Section 3 outlines the optimization issues dealt with in this work. A few numerical examples are presented in section 4. Section 5 concludes the paper.

2. THE MODEL

The configuration of the sandwich panel used in this paper is shown in Figure 1. The main focus of this study is to select a core material and/or geometry such that the vibration from the top skin is transformed as much as possible into shear deformation and in-plane wave in the core so that the deflection of the bottom skin is reduced, which results in a reduction of the sound transmission across the sandwich. The transformation of the deflection into the shear or in-plane motion is heavily influenced by the anisotropy of the material. In order to demonstrate this, a higher order model of a sandwich beam is needed. A brief overview of this model is presented in this section. Further details on the model can be found in references [23–26].

2.1. DISPLACEMENTS OF THE SKINS AND THE CORE

The skin of sandwich structures is typically very thin as compared to the core. Hence, the Euler beam theory is used to model the skin displacements. The co-ordinate system used is as follows: let x be the co-ordinate along the length of the beam, y the co-ordinate along the width and z the co-ordinate along the thickness. The displacement in the x direction is given by U and that in the z direction is denoted by W. Subscripts $i = 1, 2, 3$ are used to refer the bottom skin, core and top skin of the structure respectively.

The displacements of the core are assumed to vary in the z direction as well as in the x direction, and have to satisfy the continuity conditions at the interfaces with the skins. The

normal stress σ_x and the shear stress σ_{xz} derived from these displacements also have to satisfy equilibrium conditions at the interfaces:

$$W_2\left(x, -\frac{h_c}{2}, t\right) = W_1(x, t), \qquad W_2\left(x, \frac{h_c}{2}, t\right) = W_3(x, t),$$

$$U_2\left(x, -\frac{h_c}{2}, t\right) = U_1(x, t), \qquad U_2\left(x, \frac{h_c}{2}, t\right) = U_3(x, t), \tag{1}$$

$$\sigma_{z2}\left(x, -\frac{h_c}{2}\right) = \sigma_{z1}(x), \qquad \sigma_{z2}\left(x, \frac{h_c}{2}\right) = \sigma_{z3}(x),$$

$$\sigma_{xz2}\left(x, -\frac{h_c}{2}\right) = \sigma_{xz1}(x), \qquad \sigma_{xz2}\left(x, \frac{h_c}{2}\right) = \sigma_{xz3}(x), \tag{2}$$

where h_c refers to the thickness of the core.

The common assumption for thin middle layers that the displacements are a linear function of z [27] does not provide enough degree of freedom to satisfy all the interfacial conditions. Consequently, we have assumed that the displacement fields in the core are cubic polynomials of the thickness co-ordinate z according to the higher order theory of sandwich panels [28–32]. Such a cubic variation through the thickness provides enough degrees of freedom to satisfy all the displacement continuity and force balance conditions at the skin-core interface:

$$U_2(x, z, t) = b_0(x, t) + b_1(x, t)z + b_2(x, t)z^2 + b_3(x, t)z^3, \tag{3}$$

$$W_2(x, z, t) = c_0(x, t) + c_1(x, t)z + c_2(x, t)z^2 + c_3(x, t)z^3, \tag{4}$$

The unknown functions $b_i(x, t)$ and $c_i(x, t)$ in the above displacement expressions are then determined from equations (1) and (2).

It should be noted that the validity of this higher order sandwich model has been adequately demonstrated in the literature [28–34]. This model provides a reliable basis to demonstrate the validity of the present research concept.

2.2. CONSTITUTIVE RELATION

The constitutive relation which relates the stresses and stains in the beam is given by

$$\begin{bmatrix} \sigma_x \\ \sigma_y \\ \sigma_z \\ \sigma_{yz} \\ \sigma_{xz} \\ \sigma_{xy} \end{bmatrix} = \begin{bmatrix} Q_{11} & Q_{12} & Q_{13} & Q_{14} & Q_{15} & Q_{16} \\ Q_{21} & Q_{22} & Q_{23} & Q_{24} & Q_{25} & Q_{26} \\ Q_{31} & Q_{32} & Q_{33} & Q_{34} & Q_{35} & Q_{36} \\ Q_{41} & Q_{42} & Q_{43} & Q_{44} & Q_{45} & Q_{46} \\ Q_{51} & Q_{52} & Q_{53} & Q_{54} & Q_{55} & Q_{56} \\ Q_{61} & Q_{62} & Q_{63} & Q_{64} & Q_{65} & Q_{66} \end{bmatrix} \begin{bmatrix} \varepsilon_x \\ \varepsilon_y \\ \varepsilon_z \\ \varepsilon_{yz} \\ \varepsilon_{xz} \\ \varepsilon_{xy} \end{bmatrix}, \tag{5}$$

where the symmetric matrix $\mathbf{Q}$ is defined for the skins and the core individually assuming anisotropy for all the matrials. All variations in the y direction are neglected for a beam. As a result, Q_{15} and Q_{35} are the two normal-to-shear coupling elements which are present in the beam model. Specifically for the vibration of the sandwich beam, these terms couple the longitudinal displacement in the x direction and the normal deflection in the z direction to

the shear deformation in the xz plane. Note that there are natural materials that have this coupling property [35]. Furthermore, by using fiber reinforced composite manufacturing technology, such a coupling property can be introduced artifically in the structure [36–39].

2.3. GOVERNING EQUATION

The modal governing equations for the sandwich beam can be derived by following the Lagrange's approach [40] with the sandwich model:

$$\mathbf{M}\ddot{\mathbf{a}} + \mathbf{C}\dot{\mathbf{a}} + \mathbf{K}\mathbf{a} = \mathbf{f}, \tag{6}$$

where the matrices **M**, **C** and **K** are the mass, damping and stiffness matrices respectively. The elements of the modal force vector **f** are derived from the total work done by the external excitation which is assumed to act on the top skin only. The vector **a** consists of the generalized co-ordinates.

2.4. SOUND TRANSMISSION LOSS

An external excitation in the form of a plane sound wave of frequency ω is assumed to be normally incident on the top skin. The beam acts as a partition in the air of specific acoustic impedance ρc, where ρ and c are the density and speed of sound in the air. A sound transmission coefficient τ_s is defined as the ratio of the transmitted to incident sound intensity [41]. Also, a sound transmission loss, STL, is defined which is the common index for sound transmission measurements:

$$\tau_s = \frac{\frac{1}{2}\,\mathrm{Re}\int_0^L p_{tran}\,\dot{W}_1^*\,\mathrm{d}x}{\frac{1}{2}\,\mathrm{Re}\int_0^L p_{inc}\,\dot{W}_3^*\,\mathrm{d}x}, \quad STL = 10\log_{10}\left(\frac{1}{\tau_s}\right), \tag{7, 8}$$

where p_{inc} and p_{tran} are the incident and transmitted sound pressure fields and L is the length of the beam.

3. THE OPTIMIZATION PROBLEM

To optimally design a structure so that its STL is minimal, we have to deal with a multivariable constrained non-linear optimization problem. The optimization problem can be stated as

$$\min f(\mathbf{x}) = -STL(\mathbf{x}), \quad \mathbf{x} = [x_1, x_2, \ldots, x_n], \quad \mathbf{x} \in R^n, \tag{9}$$

$$\text{s.t.} \quad g_i(\mathbf{x}) = 0, \quad i = 1, \ldots, m, \tag{10}$$

$$c_i(\mathbf{x}) \leqslant 0, \quad i = m+1, \ldots, p, \tag{11}$$

where the g_i are m equality constraints, and the c_i are $(p-m)$ inequality constraints. $f(\mathbf{x})$ is the objective function to be minimized with respect to the vector **x** of the design variables.

In the first example of this paper, we study the optimization problem of the beam with respect to the geometric and material properties of the core. The design variables for this problem are chosen as

$$\mathbf{x} = [Q_{c15}, Q_{c35}, \rho_c, h_c], \quad \mathbf{x}_{lb} \leqslant \mathbf{x} \leqslant \mathbf{x}_{ub}, \tag{12}$$

where Q_{c15} and Q_{c35} are the two contributing coupling parameters in the core, ρ_c is the mass density of the core and h_c is the core thickness. $\mathbf{x}_{lb}$ and $\mathbf{x}_{ub}$ are vectors which define the lower and upper bounds of the design variables. Since the weight of the sandwich structure is an important concern in most applications, a constraint is introduced as follows:

$$c_1(\mathbf{x}) = \rho_c h_c L - m_0 \leqslant 0, \tag{13}$$

where m_0 is a constant and refers to the mass per unit width of an orthotropic core. A beam with such a core is considered as the base line for comparison of the results.

Other important constraints imposed are the positive definiteness of the mass matrix $\mathbf{M}$ and the semi-positive definiteness of the stiffness matrix $\mathbf{K}$.

3.1. LAGRANGE–NEWTON METHOD

There exist a large number of optimization techniques for different problems. An overview of the Lagrange–Newton method used in this paper is given next. Further details of this method can be found in references [42, 43].

First, consider the optimization problem subject to equality constraints

$$\min f(\mathbf{x}), \quad \mathbf{x} \in R, \qquad \text{subject to } g_i(\mathbf{x}) = 0, \quad i = 1, \ldots, m. \tag{14}$$

A Lagrangian is defined to incorporate the constraints,

$$L(\hat{\mathbf{x}}) = f(\mathbf{x}) + \lambda^{\mathrm{T}} \mathbf{g}(\mathbf{x}), \tag{15}$$

where $\hat{\mathbf{x}} = [\mathbf{x}, \lambda]^{\mathrm{T}}$ and $\lambda \in R^m$ is a set of Lagrange multipliers. $\mathbf{g}(\mathbf{x})$ is the vector function consisting of the constraints $g_i(\mathbf{x})$. The necessary condition for optimality of $L(\hat{\mathbf{x}})$ with respect to $\hat{\mathbf{x}}$ is

$$\nabla L(\hat{\mathbf{x}})|_{\hat{\mathbf{x}}^*} = \begin{bmatrix} f_{\mathbf{x}} + \mathbf{g}_{\mathbf{x}}^{\mathrm{T}} \lambda \\ \mathbf{g} \end{bmatrix}_{\hat{\mathbf{x}}^*} = 0. \tag{16}$$

This equation is highly non-linear in terms of the design variables $\mathbf{x}$. The optimal solution $\hat{\mathbf{x}}^*$ has to be obtained numerically by iterative methods. To start the iterative process, we pick an initial value: $\hat{\mathbf{x}}^0 = [\mathbf{x}^0, \lambda^0]^{\mathrm{T}}$. The estimation of the solution $\hat{\mathbf{x}}^*$ at the nth step can be updated by the following equation:

$$\hat{\mathbf{x}}^n = \hat{\mathbf{x}}^{(n-1)} + \begin{bmatrix} \alpha(x) & 0 \\ 0 & \beta(n) \end{bmatrix} \delta\hat{\mathbf{x}}^n, \tag{17}$$

where $\delta\hat{\mathbf{x}}^n = [\delta\mathbf{x}^n, \delta\lambda^n]^{\mathrm{T}}$ is known as the increment vector. $\alpha(n)$ and $\beta(n)$ are known as adaptation gains, where $\beta(n)$ is often taken to be unity. To improve the convergence of the method, the gain $\alpha(n)$ is selected to ensure that the new estimate $\mathbf{x}^n$ is an improved solution in the sense that it leads to a decrease of a penalty function $P(\mathbf{x}^n, \mathbf{r}^n) < P(\mathbf{x}^{(n-1)}, \mathbf{r}^{(n-1)})$, where

$$P(\mathbf{x}, \mathbf{r}) = f(\mathbf{x}) + \sum_{i=1}^{m} r_i |g_i(\mathbf{x})| + \sum_{i=m+1}^{p} r_{m+i} \max(0, c_i(\mathbf{x})). \tag{18}$$

Note that the penalty function contains the effect of inequality constraints $c_i(\mathbf{x})$. The vector $\mathbf{r}$ consists of the penalty parameters r_i for the purpose of proper weighting. A good choice for the penalty parameters is

$$r_i^n = \max\left(|\lambda_i^{(n-1)}|, \tfrac{1}{2}\left(|\lambda_i^{(n-1)}| + r_i^{(n-1)}\right)\right), \tag{19}$$

where $r_i^{(n-1)}$ is the penalty parameter at the $(n-1)$th iteration with $r_i^0 = 0$, and λ_i^n is the ith component of the vector λ at the nth iteration [42].

Expanding $\nabla L(\hat{\mathbf{x}}^n)$ in a Taylor series about $\hat{\mathbf{x}}^{(n-1)}$ and keeping the first order terms only, we have

$$\nabla L(\hat{\mathbf{x}}^n) = \nabla L(\hat{\mathbf{x}}^{(n-1)}) + \mathbf{H}(\hat{\mathbf{x}}^{(n-1)})\delta\hat{\mathbf{x}}^n + \cdots, \tag{20}$$

where the Hessian matrix $\mathbf{H}$ is defined as

$$\mathbf{H} = \begin{bmatrix} L_{\mathbf{xx}} & \mathbf{g}_{\mathbf{x}}^{\mathrm{T}} \\ \mathbf{g}_{\mathbf{x}} & 0 \end{bmatrix}, \quad L_{\mathbf{xx}} = \nabla^2 f + \sum_{i=1}^{m} \lambda_i \nabla^2 g_i. \tag{21}$$

Since the optimal value $\hat{\mathbf{x}}^*$ makes the gradient $\nabla L(\hat{\mathbf{x}}^*)$ vanish, we set $\nabla L(\hat{\mathbf{x}}^n)$ to zero leading to an equation for determining the increment $\delta\hat{\mathbf{x}}^n$. Note that the Hessian matrix is clearly singular. The increment vector $\delta\hat{\mathbf{x}}^n$ is obtained from equation (20) by using a pseudo-inverse of the Hessian matrix.

The stability and convergence of the Lagrange–Newton method has been extensively studied in the literature. For further readings, the reader is referred to the references cited earlier.

4. NUMERICAL RESULTS

Extensive numerical simulations have been carried out to study the optimization problem of a simply supported sandwich beam. The top and bottom skins of the sandwich are assumed to be identical and made of graphite/epoxy. The core material is Klegecell foam. The material constants for the skins are $Q_{s11} = 1{\cdot}67 \times 10^{10}\,\mathrm{N/m^2}$, $Q_{s13} = 5{\cdot}0 \times 10^{9}\,\mathrm{N/m^2}$, $Q_{s33} = 1{\cdot}08 \times 10^{10}\,\mathrm{N/m^2}$, $Q_{s55} = 6{\cdot}4 \times 10^{9}\,\mathrm{N/m^2}$ and the mass density is $1760\,\mathrm{kg/m^3}$. The material constants for the core are $Q_{c11} = 1{\cdot}3 \times 10^{8}\,\mathrm{N/m^2}$, $Q_{c13} = 5{\cdot}2 \times 10^{7}\,\mathrm{N/m^2}$, $Q_{c33} = 0{\cdot}8 \times 10^{8}\,\mathrm{N/m^2}$ and $Q_{c55} = 5{\cdot}0 \times 10^{7}\,\mathrm{N/m^2}$. The acoustic medium on either sides of the beam is air with $\rho = 1{\cdot}023\,\mathrm{kg/m^3}$ and $c = 330\,\mathrm{m/s}$. In this study, the skins are assumed to be orthotropic and the core material is assumed to be anisotropic. The coupling parameters used in the numerical studies, however, are not based on any actual material properties at this time. A uniform acoustic pressure acting on the top skin of the sandwich is considered as the external acoustic excitation. The beam is 2 m long. The two different optimization problems solved in this paper are discussed in the following sections.

4.1. OPTIMIZATION WITH RESPECT TO THE PROPERTIES OF THE CORE

The structure is first optimized with respect to the geometric and material properties of the core. The top and bottom skins are both assumed to be orthotropic and 5 mm thick. The properties of the skins remain unchanged in the optimization. The results of the optimized beam are compared with those of a base line beam made of the same skins and an orthotropic core with $Q_{c15} = Q_{c35} = 0$, $\rho_c = 130\,\mathrm{kg/m^3}$ and $h_c = 50\,\mathrm{mm}$. The mass per unit length of the core of the base line beam is $m_0 = 13\,\mathrm{kg/m}$.

We have minimized the objective function in equation (9) subject to the constraint in equation (13). The results, however, lead to a structure with a lower stiffness than the base line beam. To prevent the softening effect from occurring due to optimization, we introduce an additional term in the objective function:

$$\min f(\mathbf{x}) = (1-\eta)(-STL(\mathbf{x})) + \eta(f_{01} - f_1(\mathbf{x})), \tag{22}$$

where $f_1(\mathbf{x})$ is the first resonant frequency of the optimized beam, $f_{01} = 70$ Hz is the first resonant frequency of the base line beam, and η is a weighting constant. Note that the first resonant frequency of a structure is a common measure of the stiffness of the structure. This modified objective function will penalize the reduction of the stiffness of the structure.

The optimization is then performed at three discrete frequencies: 50, 100 and 500 Hz. The results shown in this paper are for an equal weighting of $\eta = 0{\cdot}5$ given to both the sound transmission loss and the stiffness of the structure. The optimization results for other values of η are similar, and are not presented. Table 1 shows the results of the optimized beam at these frequencies. Figure 2 shows the sound transmission loss STL of the optimized beam with the parameters in Table 1. These results are compared with the STL of the base line beam with an orthotropic core. It is observed that the presence of anistropic material coupling in the core is an important factor for the enhancement of the sound transmission loss across the sandwich beam, especially at lower frequencies.

The results shown in Table 1 and Figure 2 are the beam optimized at discrete frequencies. It is also common to optimize a frequency-weighted average of the transmission loss [19, 20]. In this case, the objective function is modified as

$$\min f(\mathbf{x}) = (1-\eta)(-STL_{avg}(\mathbf{x})) + \eta(f_{01} - f_1(\mathbf{x})), \tag{23}$$

where

$$\tau_{avg}(\mathbf{x}) = \sum_{i=1}^{N_f} \bar{\eta}_i \tau_{si}(\mathbf{x}), \qquad STL_{avg}(\mathbf{x}) = -10\log_{10}|\tau_{avg}(\mathbf{x})|. \tag{24}$$

$\bar{\eta}_i$ represent weighting constants and N_f is the number of frequencies. $\bar{\eta}_i$ are normalized so that the sum of all the coefficients is unity. The weighting constants $\bar{\eta}_i$ are commonly chosen to correspond to either an A-weighting or a C-weighting scale [20, 44].

The normalized A-weighting coefficients at frequencies 50, 100 and 500 Hz are 0·0019, 0·0250 and 0·9730 respectively [44]. The C-weighting scale, on the other hand, is flat over most of the audible frequency range. The normalized C-weighting coefficients at the same freuqencies are: 0·2764, 0·3480 and 0·3756 [44]. Figure 3 shows that STL curves of an A-weighted and a C-weighted optimized beam. The results are once again compared with the STL of the base line beam. It is observed from Figures 2 and 3 that the results of the

TABLE 1

Results of optimization with respect to the core properties at different frequencies. m_c refers to the mass per unit length of the core of the optimized beam. $\eta = 0{\cdot}5$ for this case

Frequency (Hz)	Q_{c15} (N/m^2)	Q_{c35} (N/m^2)	ρ_c (kg/m^3)	h_c (mm)	m_c (kg/m)	ω_1 (Hz)	ΔSTL (dB)
50	1×10^7	$2{\cdot}28 \times 10^5$	100·01	50·0	10·03	72·18	17·71
100	$7{\cdot}87 \times 10^6$	$3{\cdot}53 \times 10^5$	100·00	50·0	10·01	72·15	13·04
500	0·00	0·00	100·00	50·0	10·01	72·19	0·85

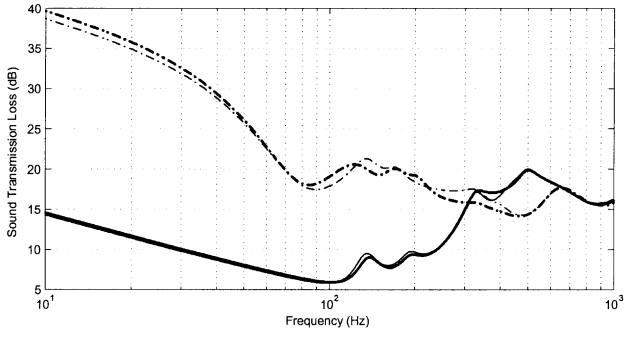

Figure 2. The variation of the STL with frequency. The —— line represents the variation of the base line beam with an orthotropic core. The – – – – line refers to the STL of the beam optimized at 50 Hz with $\eta = 0{\cdot}5$. The – – – line is at 100 Hz, and the —— line is at 500 Hz.

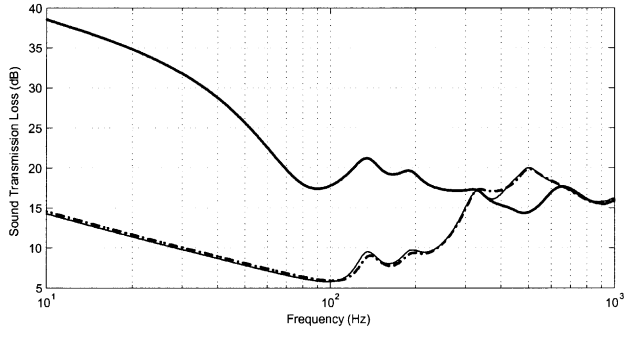

Figure 3. The —— line represents the STL of the base line beam. The STL of an A-weighted optimized beam with $Q_{c15} = Q_{c35} = 0$, $\rho_c = 100{\cdot}00$ kg/m^3 and $h_c = 50{\cdot}0$ mm is shown by the – – – – line. The STL of a C-weighted optimized beam with $Q_{c15} = 1 \times 10^7$ N/m^2, $Q_{c35} = 6{\cdot}32 \times 10^4$ N/m^2, $\rho_c = 100{\cdot}01$ kg/m^3 and $h_c = 50{\cdot}0$ mm is represented by the —— line. The weighting constant is chosen as $\eta = 0{\cdot}5$ in both cases.

A-weighted optimized beam are similar to the results obtained by optimization at the single frequency of 500 Hz. This is attributed to the trend of the A-weighting scale.

4.2. OPTIMIZATION WITH RESPECT TO GEOMETRIC PARAMETERS

In the second example, the thicknesses of all the layers of the sandwich structure are optimized for better sound transmission properties. The thicknesses of the top and bottom skins and the core of the sandwich, h_t, h_b and h_c, are considered as the design variables. The total thickness of the beam is assumed to be constant, which leads to an equality constraint,

$$g_1(\mathbf{x}) \equiv h_0 - (h_t + h_c + h_b) = 0, \tag{25}$$

where h_0 is the total thickness of the beam. In this example, we assume $h_0 = 60$ mm. A constraint on the total weight of the structure is also imposed as

$$c_1(\mathbf{x}) = (\rho_t h_t + \rho_c h_c + \rho_b h_b)L - m_0 \leqslant 0, \tag{26}$$

where $m_0 = 48{\cdot}2$ kg/m is the mass per unit length of the beam with orthotropic skins and an anisotropic core. The properties of the base line beam are specified as follows. In addition to other properties of the core specified at the beginning of the section, we also choose

TABLE 2

Results of optimization with respect to the thicknesses of the skins and the core at different frequencies. m refers to the mass per unit length of the optimized beam and $\eta = 0{\cdot}5$

Frequency (Hz)	h_t (mm)	h_c (mm)	h_b (mm)	m (kg/m)	ω_1 (Hz)	ΔSTL (dB)
50	1·2	50·0	8·8	48·22	70·42	15·03
100	1·5	50·0	8·5	48·21	70·34	14·71
500	1·0	50·0	9·0	48·20	70·44	5·48

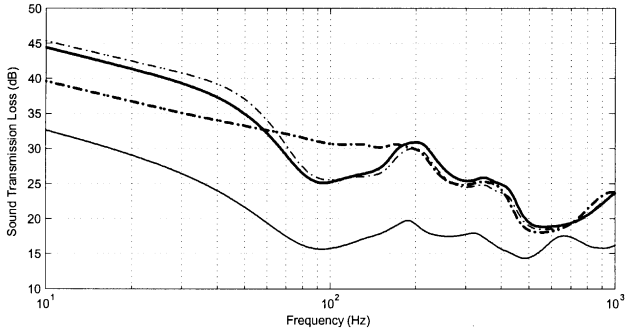

Figure 4. The variation of the STL with frequency. The —— line represents the STL of the base line beam with $h_t = h_b = 5$ mm and $h_c = 50$ mm. The – – – – line refers to the STL of the beam with optimized thicknesses for a frequency of 50 Hz. The – – – line is for 100 Hz and the —— line is for 500 Hz. Note that $\eta = 0{\cdot}5$ for all the optimization cases.

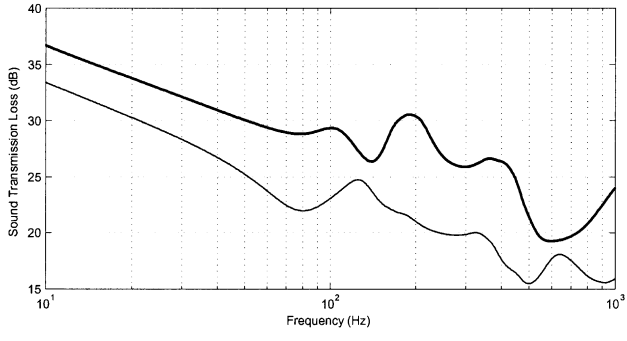

Figure 5. The —— line represents the STL of the base line beam with $h_t = h_b = 5$ mm and $h_c = 50$ mm. The STL of a C-weighted optimized beam with $h_t = 1{\cdot}0$ mm, $h_b = 9{\cdot}0$ mm and $h_c = 50{\cdot}0$ mm is shown by —— line with $\eta = 0{\cdot}5$. The results for an A-weighted optimized beam are almost exactly the same as that of the C-weighted beam in this example.

$Q_{c15} = 1 \times 10^7\ \mathrm{N/m^2}$, $Q_{c35} = 0$, $\rho_c = 130\ \mathrm{kg/m^3}$ and $h_c = 50$ mm. The orthotropic skins have the same material properties as defined earlier and $h_t = h_b = 5$ mm. All the properties of the layers of the sandwich are kept fixed in the optimization except for their thicknesses. The positive and semi-positive definiteness of the mass and stiffness matrices are also imposed as constraints on the system.

The objective function is the same as that in equation (22), with $\eta = 0{\cdot}5$ and $f_{01} = 70$ Hz, where f_{01} is the first resonant frequency of the base line beam defined above. The optimization is performed at the same discrete frequencies as before: 50, 100 and 500 Hz. The results are tabulated in Table 2.

An interesting observation can be made from the above results: in order to have better sound transmission properties, the top skin on the incident side should be much thinner than the bottom skin. The core is usually made thick enough to provide more shearing motion and acoustic damping. This is seen at all frequencies, though we show only a few results here. The STLs of the optimized beam are shown in Figure 4. The results are compared with the base line beam. The optimization results for an A-weighted and a C-weighted average of the transmission loss are presented in Figure 5. It is interesting to point out that the results for both the A-weighted and C-weighted optimized beam are exactly the same in this example. The results clearly show that it is better to construct the sandwich with a thinner skin on the incident side and a thicker skin on the other side. Further physical explanation and experimental validation of this result should be conducted in the future.

4.3. A VARIATION OF THE OBJECTIVE FUNCTION

The objective functions given by equations (22) and (23) do not allow for softening of the structure. In some applications, however, a small amount of softening in the structure might not be as critical. To this end, the objective functions can be modified by replacing $f_{01} - f_1(\mathbf{x})$ with its absolute value $|f_{01} - f_1(\mathbf{x})|$.

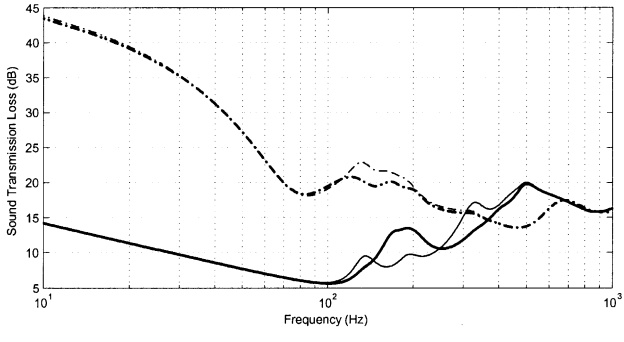

Figure 6. The variation of the STL with frequency. The —— line represents the STL of the base line beam with an orthotropic core. The – – – line refers to the STL of the beam optimized at50 Hz. The ——— line is at 100 Hz, and the —— line is at 500 Hz. In all the optimizations, the modified objective function is used with $\eta = 0{\cdot}75$.

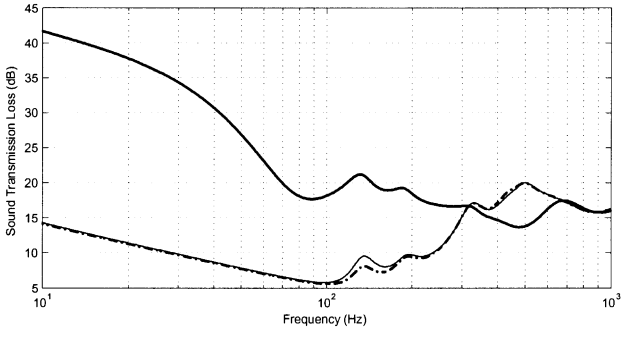

Figure 7. The —— line represents the STL of the base line beam. The STL of an A-weighted optimized beam with $Q_{c15} = 5{\cdot}38 \times 10^5$, $Q_{c35} = 1{\cdot}01 \times 10^4$, $\rho_c = 130{\cdot}01\ \mathrm{kg/m^3}$ and $h_c = 49{\cdot}7$ mm is shown by the – – – –. The STL of a C-weighted optimized beam with $Q_{c15} = 1 \times 10^7\ \mathrm{N/m^2}$, $Q_{c35} = 0$, $\rho_c = 100{\cdot}00\ \mathrm{kg/m^3}$ and $h_c = 47{\cdot}7$ mm is represented by the —— line. In both the cases, the modified objective function is used with $\eta = 0{\cdot}75$.

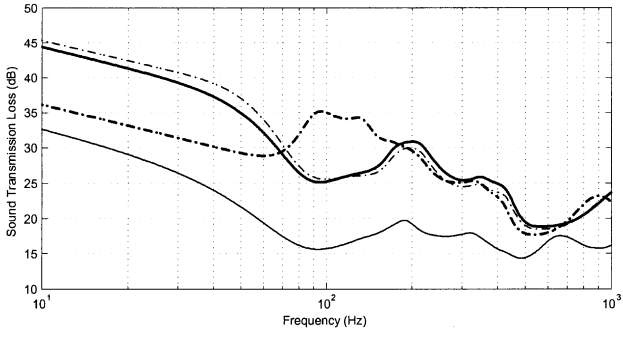

Figure 8. The —— line represents the STL curve of the base line beam with $h_t = h_b = 5$ mm and $h_c = 50$ mm. The – – – – line refers to the STL of the beam with optimized thicknesses for a frequency of 50 Hz with the modified objective function and $\eta = 0{\cdot}75$. The – – – line shows the variation for 100 Hz and the —— line for 500 Hz with the same objective function and η.

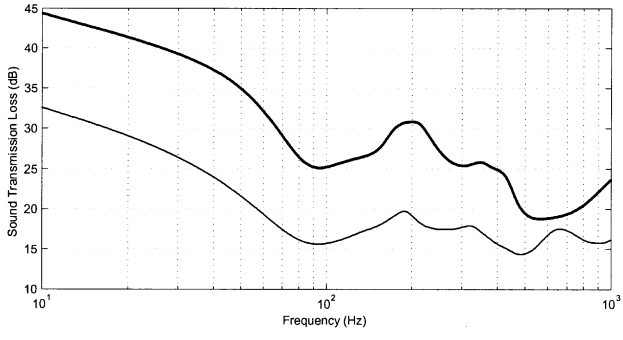

Figure 9. The —— line represents the STL of the base line beam with $h_t = h_b = 5$ mm and $h_c = 50$ mm. The STL of a C-weighted optimized beam with $h_t = 1{\cdot}0$ mm, $h_b = 9{\cdot}0$ mm and $h_c = 50{\cdot}0$ mm is shown by – – – line. The results for an A-weighted optimized beam are almost exactly the same as that of the C-weighted beam in this example. In both cases, the modified objective function is used with $\eta = 0{\cdot}75$.

TABLE 3

Results of optimization of the modified objective function with respect to the core properties at different frequencies with $\eta = 0{\cdot}75$. m_c refers to the mass per unit length of the core of the optimized beam

Frequency (Hz)	Q_{c15} (N/m^2)	Q_{c35} (N/m^2)	ρ_c (kg/m^3)	h_c (mm)	m_c (kg/m)	ω_1 (Hz)	ΔSTL (dB)
50	$9{\cdot}99 \times 10^6$	$8{\cdot}72 \times 10^5$	100·15	48·0	9·62	69·98	19·14
100	$7{\cdot}79 \times 10^6$	$3{\cdot}29 \times 10^5$	100·28	47·8	9·59	70·00	13·45
500	$7{\cdot}02 \times 10^6$	$6{\cdot}28 \times 10^5$	127·67	49·7	12·69	70·00	0·25

The modified objective function allows a slight softening of the structure, while the sound transmission loss is maximized. With this objective function, however, the optimization results vary significantly with the weighting constant η. For small values of η, for example, $\eta < 0{\cdot}6$, the optimized beam is softer than the base line beam. We have found that there is no softening at $\eta = 0{\cdot}75$. The optimization results for this case are shown in Tables 3 and 4. Figures 6–9 present the STL of the optimized beams. These results only bear small differences from those of the previous examples.

TABLE 4

Results of optimization of the modified objective function with respect to the thicknesses of the skins and the core at different frequencies with $\eta = 0{\cdot}75$. *m refers to the mass per unit length of the optimized beam*

Frequency (Hz)	h_t (mm)	h_c (mm)	h_b (mm)	m (kg/m)	ω_1 (Hz)	ΔSTL (dB)
50	1·2	50·0	8·8	48·22	70·42	15·03
100	1·8	50·0	8·2	48·21	70·37	19·04
500	1·0	50·0	9·0	48·21	70·44	5·48

5. CONCLUDING REMARKS

The optimization study of sound transmission across a sandwich beam has been presented in this paper. A detailed higher order model of a sandwich beam is used for the analysis. The Lagrange–Newton method has been used as the optimization algorithm. The main objective of the optimization is to maximize the sound transmission loss across the structure subject to the stiffness constraint, the weight constraint, and the thickness constraint. The optimization study with respect to the anisotropic coupling properties of the core of the sandwich indicates that optimal sound transmission loss can be achieved with the help of the material anisotropy. It is noted here that there are natural materials that have this property [35]. Also, fiber reinforced composite manufacturing technology can be used to artifically introduce such properties in the structure [36–39]. The optimization with respect to the thicknesses of the layers of the sandwich has discovered that better sound transmission characteristics are obtained if the skin on the incident side is much thinner than the skin on the other side. The results of this paper will provide a foundation for the design of optimal sandwich structures with enhanced sound transmission characteristics.

ACKNOWLEDGMENTS

This work is supported by a grant (F49620-98-1-0384) from the Air Force Office of Scientific Research.

REFERENCES

1. V. F. HUMPHREY and P. A. CHINNERY 1993 in *Proceedings of the Ultrasonics International Conference*, pp. 387–390. Anisotropy in the acoustic transmission properties of fibre-reinforced laminates: theoretical prediction and experimental observation.
2. T. W. TAYLOR and A. H. NAYFEH 1997 *Journal of Applied Mechanics, Transactions American Society of Mechanical Engineers* **64**, 132–138. Damping characteristics of laminated thick plates.
3. A. M. VINOGRADOV 1999 *Journal of Advanced Materials* **31**, 3–8. Material tailoring effects on buckling of asymmetric laminated beam-columns.
4. J. R. VINSON and S. SHORE 1971 *Journal of Aircraft* **8**, 843–847. Minimum weight web core sandwich panels subjected to uniaxial compression.
5. J. R. VINSON 1986 *American Institute of Aeronautics and Astronautics Journal* **24**, 1690–1696. Optimum design of composite honeycomb sandwich panels subjected to uniaxial compression.
6. J. R. VINSON 1986 in *Proceedings of the 23rd Annual Society of Engineering Science Meeting*. Minimum weight honeycomb core composite sandwich panels subjected to in-plane shear loads.
7. J. R. VINSON and A. J. LOVEJOY 1992 in *Proceedings of the Sixth Japan–US Conference on Composite Materials*. Minimum weight foam core sandwich shells under axial compression.

8. N. C. HUANG and C. Y. SHEU 1969 *AFOSR Scientific Report* 69-2136*TR*, *University of California, San Diego*. Optimal design of elastic circular sandwich beams for minimum compliance.
9. A. YOSHII 1992 *Advances in Composite Materials* **2**, 289–305. Optimum design of advanced sandwich composite using foam core.
10. A. D. BELEGUNDU and R. R. SALAGAME 1995 *Microcomputers in Civil Engineering* 301–306. Optimization of laminated ceramic composites for minimum residual stress and cost.
11. R. GRANDHI 1993 *American Institute of Aeronautics and Astronautics Journal* **31**, 2296–2303. Structural optimization with frequency constraints—a review.
12. J. S. MOH and C. HWU 1997 *American Institute of Aeronautics and Astronautics Journal* **35**, 863–868. Optimization for buckling of composite sandwich plates.
13. M. OSTWALD 1990 *Computers and Structures* **37**, 247–257. Optimum weight design of sandwich cylindrical shells under combined loads.
14. R. R. SALAGAME, A. D. BELEGUNDU and M. F. AMATEAU 1993 *SAE Special Publications*, pp. 95–99. Optimization of laminated ceramic composites for minimum thermal residual stresses.
15. G. SUN 1987 *Technical Report* 0082-5263, *University of Toronto, Institute for Aerospace Studies*. Optimization of laminated cylinders for buckling.
16. H. YAMAKAWA and A. OKUMURA 1976 *Bulletin of the JSME* **19**, 1458–1466. Optimum design of structures with regard to their vibrational characteristics. Part 1: a general method of optimum design.
17. C. L. DYM and M. A. LANG 1974 *Journal of the Acoustical Society of America* **56**, 1523–1533. Transmission of sound through sandwich panels.
18. C. L. DYM, C. S. VENTRES and M. A. LANG 1976 *Journal of the Acoustical Society of America* **59**, 364–366. Transmission of sound through sandwich panels: a reconsideration.
19. M. A. LANG and C. L. DYM 1974 *Journal of the Acoustical Society of America* **57**, 1481–1487. Optimal acoustic design of sandwich panels.
20. S. MAKRIS, C. L. DYM and J. SMITH *Journal of the Acoustical Society of America* **79**, 1833–1843. Transmission loss optimization in acoustic sandwich panels.
21. R. VAICAITIS and H. K. HONG 1983 in *Proceedings of American Institute of Aeronautics and Astronautics Eighth Aeroacoustics Conference*. Noise transmission through nonlinear sandwich panels.
22. G. R. LIU, J. TANI, K. WATANABE and T. OHYOSHI 1990 *Journal of Sound and Vibration* **139**, 313–324. Harmonic wave propagation in anisotropic laminated strips.
23. P. THAMBURAJ and J. Q. SUN 2001 *Journal of Vibration and Acoustics* **123**, 205–212. Effect of material and geometry on the sound and vibration transmission across a sandwich beam.
24. P. THAMBURAJ and J. Q. SUN 1999 *Journal of Sandwich Structures and Materials* **1**, 76–92. Effect of material anisotropy on the sound and vibration transmission loss of sandwich aircraft structures.
25. P. THAMBURAJ and J. Q. SUN 1998 in *Proceedings of the American Society of Mechanical Engineers International Congress and Exposition*. Recent studies of sound transmission loss of sandwich aircraft structures.
26. P. THAMBURAJ and J. Q. SUN 1999 in *Proceedings of SPIE*. Noise and vibration isolation across sandwich structures.
27. J. Q. SUN, W. BAO and R. N. MILES 1998 *Journal of Vibration and Acoustics* **120**, 353–360. Fatigue life prediction of nonlinear plates under random excitations.
28. A. BHIMARADDI 1984 *International Journal of Solids and Structures* **20**, 623–630. Higher order theory for free vibration analysis of circular cylindrical shells.
29. A. BHIMARADDI and L. K. STEVENS 1984 *Journal of Applied Mechanics* **51**, 195–199. Higher order theory for free vibration of orthotropic, homogeneous, and laminated rectangular plates.
30. A. BHIMARADDI and L. K. STEVENS 1986 *International Journal of Structures* **6**, 35–50. On the higher order theories in plates and shells.
31. H.-S. JING, K.-G. TZENG and J.-S. YOUNG 1993 in *Proceedings of International SAMPE Symposium and Exhibition*, Vol. 38, pp. 728–738. Elasticity solution of transverse normal stress in laminated anisotropic cylindrical panels.
32. K. D. JONNALAGADDA, T. R. TAUCHERT and G. E. BLANDFORD 1993 *Journal of Thermal Stresses* **16**, 265–284. High-order thermoelastic composite plate theories: an analytic comparison.
33. N. J. PAGANO 1974 *Journal of Composite Materials* **8**, 65–81. On the calculation of interlaminar normal stress in composite laminate.
34. N. J. PAGANO 1978 *International Journal of Solids and Structures* **14**, 385–400. Stress fields in composite laminates.
35. H. B. HUNTINGTON 1958 *The Elastic Constants of Crystals*. New York: Academic Press Inc.

36. T.-W. CHOU 1992 *Microstructural Design of Fiber Composites*. Cambridge: Cambridge University Press.
37. T.-W. CHOU 1989 *Journal of Materials Science* **24**, 761–783. Review: flexible composites.
38. S.-Y. LUO and T.-W. CHOU 1988 *Journal of Applied Mechanics* **55**, 149–155. Finite deformation and nonlinear elastic behavior of flexible composites.
39. S. Y. LUO and T.-W. CHOU 1990 *Proceedings of the Royal Society*, *London*, Series A**429**, pp. 569–586. Finite deformation of composites.
40. L. MEIROVITCH 1967 *Analytical Methods in Vibrations*. New York: Macmillan.
41. F. FAHY 1985 *Sound and Structural Vibration—Radiation, Transmission and Response*. New York: Academic Press.
42. S. K. AGRAWAL and B. C. FABIEN 1999 *Optimization of Dynamic Systems*. Boston, MA: Kluwer Academic Publishers.
43. J. NOCEDAL and S. J. WRIGHT 1999 *Numerical Optimization*. New York: Springer.
44. M. J. CROCKER 1998 *Handbook of Acoustics*. New York: John Wiley and Sons, Inc.